NIH Public Access
Author Manuscript
Matrix Biol. Author manuscript; available in PMC 2013 June 01.

Published in final edited form as:
Matrix Biol. 2012 June ; 31(5): 299–307. doi:10.1016/j.matbio.2012.03.002.

Bone Matrix Osteonectin Limits Prostate Cancer Cell Growth and Survival

Kristina Kapinas[1,4], **Katie M. Lowther**[1], **Catherine B. Kessler**[1], **Karissa Tilbury**[3], **Jay R. Lieberman**[2], **Jennifer S. Tirnauer**[1], **Paul Campagnola**[3], and **Anne M. Delany**[1,5]

[1]Center for Molecular Medicine, University of Connecticut Health Center, 263 Farmington Ave, Farmington, CT 06030

[2]New England Musculoskeletal Institute, University of Connecticut Health Center, 263 Farmington Ave, Farmington, CT 06030

[3]Department of Biomedical Engineering, University of Wisconsin, Madison, Madison, Wisconsin 53706

Abstract

There is considerable interest in understanding prostate cancer metastasis to bone and the interaction of these cells with the bone microenvironment. Osteonectin/SPARC/BM-40 is a collagen binding matricellular protein that is enriched in bone. Its expression is increased in prostate cancer metastases, and it stimulates the migration of prostate carcinoma cells. However, the presence of osteonectin in cancer cells and the stroma may limit prostate tumor development and progression. To determine how bone matrix osteonectin affects the behavior of prostate cancer cells, we modeled prostate cancer cell-bone interactions using the human prostate cancer cell line PC-3, and mineralized matrices synthesized by wild type and osteonectin-null osteoblasts in vitro. We developed this in vitro system because the structural complexity of collagen matrices in vivo is not mimicked by reconstituted collagen scaffolds or by more complex substrates, like basement membrane extracts.

Second harmonic generation imaging demonstrated that the wild type matrices had thick collagen fibers organized into longitudinal bundles, whereas osteonectin-null matrices had thinner fibers in random networks. Importantly, a mouse model of prostate cancer metastases to bone showed a collagen fiber phenotype similar to the wild type matrix synthesized in vitro. When PC-3 cells were grown on the wild type matrices, they displayed decreased cell proliferation, increased cell spreading, and decreased resistance to radiation-induced cell death, compared to cells grown on osteonectin-null matrix. Our data support the idea that osteonectin can suppress prostate cancer pathogenesis, expanding this concept to the microenvironment of skeletal metastases.

© 2012 Elsevier B.V. All rights reserved.

[5]Address correspondence to: Anne M. Delany, PhD, Center for Molecular Medicine, University of Connecticut Health Center, 263 Farmington Ave, Farmington, CT 06030, 860.679.8730 phone, 860.679.1258 fax, adelany@uchc.edu.
[4]Present address: Department of Cell Biology, University of Massachusetts Medical School, University of Massachusetts, Worcester, 55 Lake Avenue North, Worcester, MA 01655

Publisher's Disclaimer: This is a PDF file of an unedited manuscript that has been accepted for publication. As a service to our customers we are providing this early version of the manuscript. The manuscript will undergo copyediting, typesetting, and review of the resulting proof before it is published in its final citable form. Please note that during the production process errors may be discovered which could affect the content, and all legal disclaimers that apply to the journal pertain.

The authors have no conflict of interest.

NIH-PA Author Manuscript
NIH-PA Author Manuscript
NIH-PA Author Manuscript

NIH-PA Author Manuscript

NIH-PA Author Manuscript

NIH-PA Author Manuscript

Keywords

SPARC; Collagen; Second harmonic generation imaging; Radioresistance; Bone metastasis; Prostate cancer

1. Introduction

Prostate cancer frequently metastasizes to bone, with an incidence of up to 70% in autopsy series. In patients with advanced disease, bone metastases often cause intractable pain, with spinal cord compression due to vertebral metastases among the most devastating complications (Singh and Singh, 2005). Prostate cancer bone metastases result in mixed, heterogeneous osteoblastic and osteolytic lesions, in which the osteoblastic component most often predominates. In osteolytic lesions, cancer cells secrete proteases that destroy mechanically competent bone, as well as cytokines that promote osteoclast recruitment, causing further bone destruction (Chung et al., 2005). In osteoblastic lesions, abnormal, disorganized woven bone is deposited in the marrow spaces by fibroblast-like cells of the osteoblastic lineage (Roudier et al., 2008). While inhibition of bone remodeling by bisphosphonates decreases osteolysis, prostate cancer cells can still proliferate and elicit an osteoblastic lesion (Lee et al., 2002).

Some groups hypothesize that the bone microenvironment contains molecules that attract and retain prostate cancer cells (Berquin et al., 2005; Chung et al., 2005; Shiozawa et al., 2011). It is notable that stromal cells in the normal prostate express many bone-enriched genes including connective tissue growth factor (CTGF)1, osteonectin/Sparc (secreted protein acidic and rich in cysteine), biglycan, periostin, matrix gla protein, CXCL12/SDF-1 (chemokine (C-X-C) motif ligand 12/stromal cell derived factor 1) and growth differentiation factor 10 (Gdf10). It is possible that the expression of these bone-enriched proteins in normal prostate stroma leads to conditioning of prostatic epithelial cells to thrive in a bone-like environment, and this property might be retained upon malignant transformation (Berquin et al., 2005).

Although expressed in a variety of tissues, osteonectin is particularly abundant in bone (Robey et al., 2006; Malaval et al., 1987). This integrin-binding matricellular protein regulates collagen fibril assembly, and it can modulate cell proliferation, survival and differentiation in a cell type-specific manner (Delany and Hankenson, 2009; Bradshaw, 2009). Immunohistochemistry studies demonstrated that both normal prostate epithelial cells and primary prostate carcinomas express low to moderate levels of osteonectin. However, osteonectin expression is increased in metastatic foci (Thomas et al., 2000; Dhanasekaran et al., 2001).

Osteonectin enhances the invasive properties of multiple prostate carcinoma cell lines, and can induce matrix metalloproteinase activity in vitro (Jacob et al., 1999; Chen et al., 2007). The activation of $\alpha_v\beta_3$ and $\alpha_v\beta_5$ integrins by osteonectin was necessary for increased migration of prostate cancer cells, through a mechanism at least partially dependent on tumor cell expression of VEGF (vascular endothelial growth factor) (De et al., 2003). Further, metastatic prostate cancer cells express a secreted isoform of ErbB3 (p45-sErbB3), which interacts with cells of the osteoblastic lineage and induces the expression of osteonectin (Lin et al., 2008). This results in increased invasiveness, which can be blocked

[1]Abbreviations: chemokine (C-X-C) motif ligand 12/stromal cell derived factor 1, CXCL12/SDF-1; connective tissue growth factor, CTGF; growth differentiation factor 10, Gdf10; osteonectin/SPARC, secreted protein acidic and rich in cysteine); second harmonic generation, SHG; severe combined immunodeficiency, SCID; transgenic adenocarcinoma mouse prostate, TRAMP.

NIH-PA Author Manuscript

NIH-PA Author Manuscript

NIH-PA Author Manuscript

by osteonectin neutralizing antibodies (Chen et al., 2007). These data suggest that prostate cancer cells both produce osteonectin and induce osteonectin production in new sites, which could enhance their ability to metastasize.

Recently, the TRAMP (transgenic adenocarcinoma mouse prostate) model was used to directly test the effect of endogenous osteonectin on prostate cancer development and progression. In this model, the development of prostate adenocarcinoma is promoted by the expression of the SV40 T antigen in prostatic epithelial cells (Gingrich et al., 1996; Pienta et al., 2008). Two groups evaluated the TRAMP model in an osteonectin-null background. Osteonectin-null/TRAMP mice with a C57Bl/6 genetic background exhibited accelerated cancer development, progression, and metastasis as compared to osteonectin wild type/TRAMP controls (Said et al., 2009). A second group evaluated osteonectin-null/TRAMP mice in a mixed C57Bl/6/129 genetic background. They found that a greater proportion of osteonectin-null mice developed a more severe grade of prostate cancer, although this difference was not statistically significant, nor were differences in metastasis noted (Wong et al., 2008). While somewhat conflicting, these studies support the idea that osteonectin in the tumor and/or the stroma may limit primary prostate tumor development and progression.

However, the TRAMP model is not useful for testing the impact of osteonectin on prostate cancer skeletal metastases, as bone metastases are rare in these mice. We sought to explore the effects of bone matrix osteonectin on the behavior of prostate cancer cells by using murine osteoblasts to create normal and osteonectin-null bone matrix in vitro. Since these matrices are synthesized by bone cells, they are complex, appropriately crosslinked, mineralized and biologically relevant. We tested the impact of these matrices on the growth and survival of PC-3 cells, a human prostate cancer cell line isolated from a bone metastasis.

2. Results

2.1. Bone matrix secreted by osteonectin-null osteoblasts is disorganized and hypomineralized

Wild type and osteonectin-null mouse osteoblasts were grown on transwell filters for 4 weeks, in a differentiation medium containing ascorbic acid and β-glycerol phosphate (Delany et al., 2003). During this time, the bone cells synthesized and deposited a mineralized bone matrix with features similar to that of woven bone (Bellows et al., 1986; Kapinas et al., 2009). We used second harmonic generation (SHG) imaging to examine the fibrillar structure of the matrices, as this technique directly images supramolecular assembly. Type I collagen produces high SHG contrast without the use of exogenous stains, and the intensity of SHG signal is directly related to the square of the collagen abundance and to collagen organization (Nadiarnykh et al., 2007; LaComb et al., 2008). SHG imaging showed that the matrix synthesized by wild type osteoblasts was highly organized, whereas that synthesized by osteonectin-null cells appeared to be assembled in random networks (Figure 1A and B). The wild type matrix contained collagen fibers that were significantly longer than those in osteonectin-null matrix, with a trend toward greater SHG intensity ($p=0.07$ for osteonectin-null vs. WT) (Figure 1E and F). These data are consistent with greater collagen fiber organization in the wild type matrix. In addition, we used microCT analysis to determine the abundance of mineralization. This demonstrated that the matrices produced by osteonectin-null osteoblasts contained about 50% less mineral than the wild type matrices (mineralized volume 0.49 mm^3 for osteonectin-null vs. 0.99 mm^3 for wild type) (Figure 1C and D). These microCT data are consistent with our previous findings of decreased mineral in osteonectin-null matrices (Delany et al., 2003; Kessler and Delany, 2008).

Since the matrices synthesized in vitro could be affected by substrate and/or culture conditions, we also performed SHG imaging on sections from osteoblastic lesions created in

NIH-PA Author Manuscript

NIH-PA Author Manuscript

NIH-PA Author Manuscript

vivo. We generated osteoblastic prostate cancer lesions in SCID (severe combined immunodeficiency) mice by injecting LAPC-9 human prostate carcinoma cells intratibially (Figure 2). LAPC-9 is one of the few human prostate cancer cell lines that will elicit osteoblastic lesions when injected into the tibia of immunocompromised mice (Lee et al., 2002; Feeley et al., 2009). Eight weeks post-injection, we observed osteoblastic lesions with a woven bone phenotype, similar to that of the wild type matrices that were synthesized on transwells (compare Figures 1A, 2C, 2D). To determine how the collagen organization in the osteoblastic lesions compares to that of trabecular and cortical bone, SHG imaging was performed on bone sections from wild type mice. As expected, collagen organization in the osteoblastic lesion was more similar to that of wild type trabecular bone (Figure 2E). Moreover, these imaging studies highlighted the differences in collagen fibril organization between the trabecular and cortical bone compartments (Figures 2E and G). SHG imaging of cortical and trabecular bone from osteonectin-null mice confirmed defects in bone collagen fibril organization in the mutants (Figure 2F and H). These data suggest that the collagen organization of matrices synthesized in vitro by wild type mouse osteoblasts may model osteoblastic lesions observed in vivo, validating our use of these matrices.

To determine whether a grossly altered matrix composition might be contributing to the difference in collagen organization observed in matrix synthesized by osteonectin-null osteoblasts, we quantified the relative abundance of collagen (Figure 3A). A Sirius red dye binding assay showed that the wild type and osteonectin-null matrices contained similar amounts of acid extractable fibrillar collagen. Hydroxyproline content of the matrices was also comparable: 0.22 ± 0.03 μg hydroxyproline/μg protein for wild type vs. 0.26 ± 0.03 μg hydroxyproline/μg protein for osteonectin-null. Further, we examined levels of fibronectin, vitronectin, and tenascin C, all non-collagenous integrin binding proteins associated with metastasis (Docheva et al., 2010; Sung et al., 2008; Larsen et al., 2006; Cooper e al., 2002; Midwood and Orend, 2009). Western blot analysis showed that extracts from matrices produced by wild type and osteonectin-null osteoblasts contained similar amounts of fibronectin, vitronectin, and tenascin C (Figure 3). This is consistent with our previous findings, that wild type and osteonectin-null bones or cultured osteoblasts have similar levels of mRNA for Col1A1, and for non-collagen matrix proteins osteopontin and fibronectin (Delany et al., 2000, 2003). These data suggest that wild type and osteonectin-null bone matrix differ primarily in matrix organization, rather than fibrillar collagen content, although it is possible that minor changes in less abundant matrix components also exist.

2.2 Osteonectin-null bone matrix limits prostate cancer cell spreading

PC-3 is a human cell line derived from a prostate cancer bone metastasis, so it is a good model for determining how bone matrix may affect the behavior of bone-metastatic prostate cancer cells (Sobel and Sadar, 2005). We seeded PC-3 cells on matrices at a low density, then fixed and stained the cells with phalloidin to visualize the actin cytoskeleton, as a marker of cell morphology. We examined the cells at early time points (1–3 hours after plating) and at later time points (1–7 days after plating). Between 1 hour and 5 days post-plating, PC-3 cells displayed a rounded morphology on both wild type and osteonectin-null matrices. However, after 6–7 days of culture, we observed that cells cultured on wild type matrices were well spread, whereas the shape of the cells grown on the osteonectin-null matrices did not significantly change (Figure 4). The fibroblastic morphology of the PC-3 cells on the wild type matrix was similar to the morphology of these cells grown on a rigid surface such as tissue culture plastic. These data show that matrix organization and the presence of osteonectin affects prostate cancer cell morphology.

NIH-PA Author Manuscript

NIH-PA Author Manuscript

NIH-PA Author Manuscript

2.3 Osteonectin-null bone matrix supports proliferation and radiation-resistance

Since growth of PC-3 cells on the wild type and osteonectin-null matrices ultimately resulted in differences in cell morphology, we next assessed whether the matrices could promote differences in proliferation rate, as assessed by ^{3}H-thymidine incorporation (Figure 5A). As seen for cell morphology, growth rates on the wild type and osteonectin-null matrices were similar up to 5 days post-plating, and then diverged. At day 7, there was a plateau in the proliferation rate of PC-3 cells on the wild type matrix, whereas cells on the osteonectin-null matrix continued to proliferate. These data suggest that the osteonectin-null matrix sustained signals important for cell growth, and that continued proliferation correlated with a more rounded, less-spread morphology.

To determine whether addition of exogenous osteonectin could suppress the proliferation of PC-3 cells grown on osteonectin-null matrix, we supplemented the growth medium with recombinant human osteonectin at the time of plating. ^{3}H-thymidine incorporation assay showed that the proliferation rate of PC-3 on the osteonectin-null matrix was not affected by the addition of soluble osteonectin (Figure 5B). We then asked whether PC-3 cells, themselves, expressed osteonectin. Western blot analysis showed that osteonectin was easily detected in the conditioned medium of PC-3 cells (Figure 5C). In comparison, osteonectin in conditioned medium from the human osteosarcoma cell line MG-63 was about 3 fold more than that of PC-3 (relative band intensity 26 ± 3 for PC-3 vs. 75 ± 2 for MG-63). Interestingly, MG-63 conditioned medium contained an osteonectin doublet. The faster mobility band may represent a differentially glycosylated species, a cleavage product, or an alternate protein isoform. These data suggest that soluble osteonectin does not affect proliferation in this system.

Differences in cell shape and proliferation were observed in PC-3 cells cultured on wild-type and osteonectin-null matrices after ~7 days. To determine whether the difference in cell proliferation could be mediated by soluble factors, possibly secreted by the PC-3 cells or liberated from the osteoblast-derived matrix, we performed a conditioned medium transfer experiment. PC-3 cells were cultured on wild type or osteonectin-null matrix for 7 days. Their conditioned medium was harvested and then placed on serum-deprived PC-3 cells, plated on tissue culture plastic. Several dilutions of medium were tested, including 100% conditioned medium, 1:2 and 1:3 dilution of conditioned medium in 10% FBS. After 24 hours of treatment, cell proliferation was measured by ^{3}H-thymidine incorporation assay. This assay did not reveal significant differences in the ability of conditioned medium from cells grown on wild type or osteonectin-null matrix to stimulate cell proliferation. These data suggest that soluble factors alone may not play a role in the differences in behavior of PC-3 cells on wild type and osteonectin-null matrix.

Radiation is commonly used as a palliative therapy for prostate cancer bone metastases. Since increased cell replication in prostate cancer is associated with resistance to therapy, we next asked whether the bone matrices could differentially affect sensitivity to ionizing radiation (Zhang et al., 2010; Kong et al., 2010). PC-3 cells were grown on wild type and osteonectin-null matrices for 6 days, and then treated with single dose gamma radiation (0, 2 or 4 Gy). Cells were maintained on the matrices for an additional 2 days, then removed from the matrices and cultured on tissue culture plastic for a clonogenic survival/colony forming assay (Weidhaas et al., 2007). After 8 days of growth, colonies were stained with crystal violet and quantified. These studies showed that compared to cells grown on wild type matrix, cells grown on the osteonectin-null matrices were more resistant to 2 or 4 Gy of radiation (Figure 6). These data suggest that a bone matrix containing osteonectin may reduce the survival of prostate cancer cells exposed to radiation. It is not clear how much of this effect on proliferation and survival is due to bone matrix-associated osteonectin itself or

NIH-PA Author Manuscript

NIH-PA Author Manuscript

NIH-PA Author Manuscript

to the osteonectin-mediated changes in collagen organization, and it is likely that both mechanisms are active.

3. Discussion

There is great interest in understanding the interaction between the bone microenvironment and progression of osteoblastic and osteolytic bone metastasis. Cell-matrix interactions have profound effects on cell behavior, and can alter the response of tumor cells to therapeutics, including radiation (Mannino and Chalmers, 2011; Jean et al., 2011; Storch et al., 2010). This study is unique in that it demonstrates that bone matrix-associated osteonectin attenuated the growth of bone metastatic prostate cancer cells and increased their sensitivity to ionizing radiation (Figures 5 and 6). These observations are consistent with reports that osteonectin increases the sensitivity of colorectal cancer cells to radiation and chemotherapy (Tai et al., 2005). Although osteonectin promotes the migration of prostate cancer cells and its expression is increased in metastases, a growing body of evidence suggests that osteonectin expression by stromal cells and the prostate cancer cells themselves limits cancer growth (Thomas et al., 2000; Dhanasekaran et al., 2001; De et al., 2003; Chen et al., 2007; Said et al., 2009; McCabe et al., 2011). Our data support the concept that osteonectin may suppress prostate cancer pathogenesis, and expands this concept to the microenvironment of the skeleton, which is a major site of prostate cancer metastasis and a key mediator of patient morbidity in this disease.

3.1 A novel in vitro model for studying cancer cell – bone interactions

The structural complexity of collagen matrices in vivo is not mimicked by reconstituted collagen scaffolds or by more complex substrates, such as basement membrane extracts (i.e. Matrigel™) (Wolf et al., 2009; Poincioux et al., 2009). In our study, we examined the behavior of prostate cancer cells cultured on a multidimensional, cross-linked collagen matrix. In addition, these osteoblast-synthesized matrices contained an appropriate complement of non-collagenous matrix molecules. As such, the matrices are biologically relevant, and provide an advantage with regard to examining the effects of matrix on cell behavior. This system could be highly useful for examining additional aspects of tumor-bone matrix interactions in prostate cancer biology and the biology of other bone-metastatic tumor types.

3.2 Potential matrix-mediated mechanisms for regulation of prostate cancer cell growth and survival

Type I collagen can promote the proliferation of bone-metastatic prostate cancer cells, as well as affecting cytoskeletal organization (Moro et al., 2005; Hall et al., 2006; Docheva et al., 2010). Osteonectin is a collagen binding protein important for fibril organization, and the footprint of osteonectin on the collagen fibril overlaps both the cell interaction domain and portions of the matrix interaction domain (Di Lullo et al., 2002; Sweeney et al., 2008). It is possible that, in the absence of osteonectin, domains of the collagen fibril important for promoting growth and survival may be more accessible, providing a potential mechanism for the increased growth and survival of cells grown on the osteonectin-null bone matrix.

Organization and fibril density affect matrix rigidity, which in turn, can have a profound impact on cell phenotype (Janmey et al., 2009). The organization of collagen matrix synthesized in the absence of osteonectin was distinctly different from that of wild type matrix, suggesting that matrix rigidity may also be different (Figure 1). Tilghman et al. recently reported that the growth of PC-3 cells was not sensitive to matrix rigidity when cells were assayed for up to 5 days, using collagen coated polyacrylamide gels as a model (Tilghman et al., 2010). Similarly, we noted that PC-3 cells plated on either wild type or

NIH-PA Author Manuscript

NIH-PA Author Manuscript

NIH-PA Author Manuscript

osteonectin-null bone matrix initially displayed similar morphology and growth characteristics (Figures 4 and 5). However, we found a significant difference in cell growth and spreading after 7 days of culture. Since a differential effect of the matrix on PC-3 growth and morphology was not evident until day 7, it is likely that the cells and/or matrix undergo a complex series of changes preceding the observed differences in cell proliferation and spreading (Figures 4 and 5). Whereas collagen organization can affect matrix stiffness, which is a mechanical characteristic, it is clear that the wild type and osteonectin-null matrices also present spacial differences with regard to fibril alignment and pore size. Since surface topography affects cell shape, motility and differentiation, it is probable that the PC-3 cells can respond to the different spacial cues provided by the wild type and osteonectin-null matrices (Kim et al., 2009; Teixeira et al., 2003; Yim et al., 2005).

Osteonectin can be cleaved by metalloproteinases and cathepsin K (Podgorski et al., 2009; Sasaki et al., 1997). Since bone matrix-associated osteonectin limits prostate cancer growth and survival, it is possible that the proteolysis of osteonectin could result in a more favorable microenvironment for metastatic cells. However, proteolytic fragments of osteonectin are suggested to have biological properties that differ from that of the intact protein, including differences in collagen affinity, and cell type-specific effects on proliferation and angiogenesis (Sage et al., 2003; Sasaki et al., 1997). The effects of osteonectin fragments on the growth and behavior of prostate cancer cells have not been reported, and may play a role in suppressive activity of osteonectin on prostate cancer cells in bone.

3.3 Potential cell-mediated mechanisms for regulation of prostate cancer cell growth and survival

It is likely that the actions of osteonectin on prostate cancer cells in the bone microenvironment are both direct and indirect. Direct actions could be mediated through the effects of osteonectin on matrix structure and on cell-matrix interactions, as discussed above. In addition, it is possible that indirect effects of osteonectin, which are not addressed in this study, could be mediated through the ability of this matricellular protein to modulate the activity and fate of other cell types, including cells of the osteoblast and osteoclast lineage. For example, cells of the osteoblast lineage are an important part of the stem cell niche, and osteonectin promotes the differentiation and survival of this cell type (Delany et al., 2003; Kessler and Delany, 2008; Bianco, 2011). Since metastatic prostate cancer cells compete with hematopoietic stem cells for interaction with the skeletal niche, osteonectin could affect this interaction by affecting the differentiation and survival of niche cells (Shiozawa et al., 2011). Moreover, accentuated osteoclastogenesis is observed in osteonectin-null mice subjected to remodeling challenges, such as treatment with parathyroid hormone or the intratibial injection of a murine prostate cancer cell line (Machado do Reis et al., 2008; McCabe et al., 2011). These data suggest that osteonectin also plays a role in limiting osteoclastogenesis, important for prostate cancer skeletal metastasis.

Murine models indicate that osteonectin gene dosage effects skeletal phenotype (Machado do Reis et al., 2008). Further, haplotypes consisting of 3 single nucleotide polymorphisms (SNPs) in the 3’ untranslated region (UTR) of the osteonectin gene have been associated with bone mass in a cohort of men with idiopathic osteoporosis (Delany et al., 2008). Our recent data suggest that osteonectin 3’ UTR SNPs can mediate differential regulation of gene expression, providing one potential mechanism for variations in osteonectin expression among individuals (our unpublished data). Variations in osteonectin gene expression among prostate cancer patients may affect the ability of metastatic prostate cancer cells to grow and survive in the skeleton.

NIH-PA Author Manuscript

NIH-PA Author Manuscript

NIH-PA Author Manuscript

4. Experimental Procedures

4.1. Cell culture and synthesis of bone matrices

Wild type and osteonectin-null osteoblastic cell lines (mObI-2) were plated onto 8 μm pore size polycarbonate transwell filters (Corning, Corning, NY) or tissue culture plastic at 50,000 cells/cm^2, in α-MEM (Invitrogen, Fredrick, MD) supplemented with 10% fetal bovine serum (FBS) (Atlanta Biologicals, Norcross, GA) (Delany et al., 2003). After 7 days, the cells were maintained in α-MEM supplemented with 10% FBS, 50 μg/mL ascorbic acid and 5 mM β- glycerolphosphate. Medium was changed twice a week for 4 weeks. Osteoblastic cells were removed from the matrices by incubating transwells in 0.5% Triton X-100 in PBS for 30 minutes, followed by a 15 minute incubation in 25 mM ammonium actetate (pH 9). Matrix transwells were washed extensively with PBS, and then stored at −20°C (Gabbitas & Canalis 1989). The matrices synthesized on transwell filters remained as a sheet following treatment with detergent and ammonium acetate.

PC-3 cells were obtained from American Type Culture Collection (ATCC, Norcross VA) and maintained in F12/K medium supplemented with 10% FBS(Kaighn et al., 1979). MG63 osteosarcoma cells were also obtained from ATCC, and maintained in αMEM supplemented with 10%FBS.

4.2. Analysis of bone matrices

To image collagen fibril organization, matrix transwells were prepared as described above, fixed in buffered formalin, and briefly decalcified (Lamcomb et al., 2007). Membranes were excised, mounted on a microscope slide, and subjected to second harmonic generation (SHG) imaging (Nadiranykh et al., 2007). The SHG imaging system consisted of a laser scanning head (Olympus Fluoview 300) mounted on an upright microscope (Olympus BX61), coupled to a mode-locked Titanium Sapphire laser. All measurements were performed with a laser wavelength of 900 nm, with average power of 50 mW at the specimen. The SHG was detected in the forward direction where the excitation objective and collection lenses were a long working distance 40×0.8 N.A. water-immersion objective and a 0.9 N.A. condenser, respectively. The SHG signal was isolated with a longwave pass dichroic mirror and 10-nm bandpass filters (450 nm). The signals were detected by a pair of identical photon-counting photomultiplier modules (Hamamatsu). At least 3 slides per condition were analyzed, and 3–5 images were captured per slide.

Fiber lengths were measured using ImageJ (http://rsbweb.nih.gov/ij/index.html). The threshold function identified individual fibers and then the freehand tool determined the lengths. The threshold level was chosen based on discrimination of the SHG signal from fibrillar collagen against the background noise. In addition, average intensities were measured in Matlab. The images were thresholded to identify the pixels containing SHG signals above background noise, and the average intensity was calculated per pixel.

For Western blot analysis, matrices were homogenized in 1X sample buffer (62.5 mM Tris pH 6.8, 10% glycerol, and 2% SDS). Protein content was measured using the BioRad (Hercules, CA) *DC* Protein Assay Kit, according to the manufacturer's instructions. Equal amounts of matrix proteins were subjected to electrophoresis through a 6% SDS-polyacrylamide gel under reducing conditions, and transferred to a PVDF membrane (Millipore, Billerica, MA). Membranes were blocked with 4% nonfat milk powder plus 0.45% fish gelatin in PBST (phosphate buffered saline, 0.1% Tween) and probed with rabbit monoclonal anti-vitronectin (ab45139, Abcam), rabbit polycolonal anti-fibronectin (ab2413, Abcam) or rat monoclonal anti-tenascin C (ab6346, Abcam). Goat anti-rabbit- or goat anti-rat-horseradish peroxidase (HRP) conjugated secondary antibody (Sigma) was used, as

NIH-PA Author Manuscript

NIH-PA Author Manuscript

NIH-PA Author Manuscript

appropriate. Bands were visualized by chemiluminescence (Cell Signaling, Danvers, MA) and fluorography. Relative band intensities in scanned images were analyzed using Image J.

Osteonectin expression in PC-3 and MG-63 cells was determined by Western blot analysis. Confluent cultures were incubated in serum-free medium for 16 hours and conditioned medium has harvested. Equal amounts of serum-free conditioned medium were precipitated with ½ volume 10% trichloroacetic acid (TCA) and resuspended in 1X reducing sample buffer (sample buffer + 5% beta-mercaptoethanol). Conditioned medium were subjected to electrophoresis through a 10.5% SDS-polyacrylamide gel, and transferred to a PVDF membrane. Membranes were blocked overnight in 3% BSA in TBST (Tris-buffered saline, 0.1% Tween), and were probed with a rabbit anti-bovine osteonectin primary antibody (BON-1; gift of L. Fisher, NIDCR, NIH), followed by goat anti-rabbit-horseradish peroxidase conjugated secondary antibody (Sigma) (Ingram et al., 1993). Western blot experiments were performed at least twice, with N=3–5 in each experiment.

For analysis of acid soluble collagen content, matrices were homogenized in 0.5 M acetic acid, and equal amounts of protein were subjected to a sirius red dye binding assay, according to the manufacturer's instructions (Sircol Collagen assay, Biocolor Ltd, Accurate Chemical & Scientific Corp, Westbury, NY). For analysis of hydroxyproline content, matrices were lyophilized, and then hydrolyzed in 6 N hydrochloric acid for 3 hours at 120°C. Hydroxyproline content was determined using a chromogenic assay, following the manufacturer's instructions (BioVision, Mountain View, CA). Protein content was measured using the BioRad *DC* Protein Assay Kit. Collagen/hydroxyproline assays were performed with N=4–5.

4.3. Immunofluorescence

For analysis of cell morphology, PC-3 cells were plated on matrix transwells at 9,000 cells/cm^2. At various time points, samples were fixed in buffered formalin, permeabilized with 0.1% Triton X-100, blocked in 1% BSA in PBST and stained with Alexa Fluor 488-phalloidin conjugate and DAPI (Invitrogen). Wells were washed with PBS, matrices were excised and mounted with 0.5% *p*-phenylenediamine (Sigma-Aldrich) in 20 mM Tris 8.8 and 90% glycerol, sealed with nail polish, and stored at 4°C. Imaging was performed using a 100 1.4 NA Plan Apo objective on an inverted Nikon TE2000-U microscope (Nikon Instruments; Melville, NY) equipped with a Yokogawa CSU-10 spinning disk confocal head (Perkin Elmer; Wellesley, MA) and a deep-cooled Orca AG CCD camera (Hamamatsu Photonics; Bridgewater, NJ). Image acquisition and processing were controlled by MetaMorph software (Molecular Devices Corp.; Sunnyvale, CA). Image stacks were acquired at 0.2-μM intervals in the z-axis. ImageJ was used to quantify relative cell perimeter, and at least 40 single cells per condition per time point were analyzed.

4.4 Cell proliferation and survival assays

To monitor cell proliferation, PC-3 cells were plated on matrix transwells at 24,000 cells/cm^2. At 1, 3, 5, and 7 days post-plating, cells were pulsed with 10 μC/mL ^{3}H-thymidine for 90 minutes. Transwells were washed with PBS, and subjected to two 10 minute washes with cold 10% trichloroacetic acid (TCA). Incorporation of ^{3}H-thymidine into macromolecules was quantified by scintillation counting (Zhang et al., 2007). In selected experiments, 3 μg/mL recombinant human osteonectin (rhON, R & D Systems) was added to the PC-3 cells at the time of plating. This concentration of osteonectin has been shown to decrease the proliferation rate of pancreatic carcinoma cells (Zhivkova-Galunska et al., 2010). For the conditioned medium transfer experiments, PC-3 cells were cultured on wild type or osteonectin-null matrices for 7 days. The conditioned medium was collected, filtered

NIH-PA Author Manuscript

NIH-PA Author Manuscript

NIH-PA Author Manuscript

through a 0.45 μm filter, and then used to treat serum-deprived PC-3 cells that had been cultured on tissue culture plastic. N=4–6 per condition, per time point.

To assess radiation-induced replicative cell death, PC-3 cells were plated on matrix transwells at 24,000 cells/cm^2 and cultured for 6 days. Triplicate wells were then subjected to a single dose of 0, 2 or 4 Gy gamma radiation (Gamma Cell 40). Cells were re-fed after radiation treatment. 48 hours post-radiation, PC-3 cells were removed from matrices by treatment with collagenase, hyaluronidase and trypsin (Kalajzic et al., 2005). Equal volumes of cells were re-plated in 6 well plates, in triplicate, and cultured for an additional 8 days. Cells were then fixed in buffered formalin and stained with crystal violet. Wells were scanned and crystal violet staining was quantified using ImageJ.

4.5 Data Analysis

Data are presented as mean ± SEM. Data were analyzed by one-way ANOVA with Bonferroni post-hoc test or by Student's *t* test (KaleidaGraph, Synergy Software, Reading, PA).

Highlights

- We modeled prostate cancer cell-bone matrix interactions in vitro
- Osteonectin-null bone matrix was disorganized
- Osteonectin-null bone matrix promoted prostate cancer cell proliferation
- Osteonectin-null bone matrix promoted resistance to radiation-induced cell death
- Osteonectin may suppress prostate cancer pathogenesis in the skeletal microenvironment.

Acknowledgments

We thank Haley Goldsmith (Department of Biomedical Engineering, University of Wisconsin) for help with SHG image analysis. We thank Dr. Larry Fisher (NIDCR, National Institutes of Health) for the gift of the BON-1 antibody. We thank Dr. Doug Adams (University of Connecticut Health Center) for microCT analysis.

This study was supported by a Neag Comprehensive Cancer Center Intramural Pilot Grant from University of Connecticut Health Center, and NIH/NIAMS AR44877 (AD).

References

Bellows CG, Aubin JE, Heersche JN, Antosz ME. Mineralized bone nodules formed in vitro from enzymatically released rat calvaria cell populations. Calcif Tissue Int. 1986; 38:143–154. [PubMed: 3085892]

Berquin IM, Min Y, Wu R, Wu H, Chen YQ. Expression signature of the mouse prostate. J. Biol. Chem. 2005; 280 3644236451.

Bianco P. Bone and the hematopoietic niche: a tale of two stem cells. Blood. 2011; 19:5281–5288. [PubMed: 21406722]

Bradshaw AD. The role of SPARC in extracellular matrix assembly. J Cell Commun. Signal. 2009; 3:239–246. [PubMed: 19798598]

Chen N, Ye X-C, Chu K, Navone NM, Sage EH, Yu-Lee L-Y, Logothetis CJ, Lin S-H. A secreted isoform of ErbB3 promotes osteonectin expression in bone and enhances the invasiveness of prostate cancer cells. Cancer Res. 2007; 67:6544–6548. [PubMed: 17638862]

NIH-PA Author Manuscript NIH-PA Author Manuscript NIH-PA Author Manuscript

Chung LWK, Baseman A, Assikis V, Zhau HE. Molecular insights into prosate cancer progression: the missing link of tumor microenvironment. J. Urol. 2005; 173:10–20. [PubMed: 15592017]

Cooper CR, Chay CH, Pienta KJ. The role of $\alpha_v\beta_3$ in prostate cancer progression. Neoplasia. 2002; 3:191–194. [PubMed: 11988838]

De S, Chen J, Narizhneva NV, Heston W, Brainard J, Sage EH, Byzova TV. Molecular pathway for cancer metastasis to bone. J. Biol. Chem. 2003; 278:39044–39050. [PubMed: 12885781]

Delany AM, Amling M, Priemel M, Howe CC, Baron R, Canalis E. Osteopenia and decreased bone formation in osteonectin-deficient mice. J. Clin. Invest. 2000; 105:915–923. [PubMed: 10749571]

Delany AM, Hankenson KD. Thrombospondin-2 and osteonectin/SPARC are critical regulators of bone remodeling. J. Cell Commun. Signal. 2009; 3:227–238. [PubMed: 19862642]

Delany AM, Kalajzic I, Bradshaw AD, Sage EH, Canalis E. Osteonectin-null mutation compromises osteoblast formation, maturation, and survival. Endocrinology. 2003; 144:2588–2596. [PubMed: 12746322]

Delany AM, McMahon D, Powell JS, Greenberg DA, Kurland ES. Osteonectin/SPARC polymorphisms in Caucasian men with idiopathic osteoporosis. Osteoporos Int. 2008; 19:969–973. [PubMed: 18084690]

Dhanasekaran SM, Barrette TR, Ghosh D, Shah R, Varambally S, Kurachi K, Pienta KJ, Rubin MA, Chinnaiyan AM. Delineation of prognostic biomarkers in prostate cancer. Nature. 2001; 412:822–826. [PubMed: 11518967]

Di Lullo GA, Sweeney SM, Körkkö J, Ala-Kokko L, San Antonino JD. Mapping of the ligand-binding sites and disease-associated mutations on the most abundant protein in the human, type I collage. J. Biol. Chem. 2002; 277:4223–4231. [PubMed: 11704682]

Docheva D, Padula D, Schieker M, Clausen-Schaumann H. Effect of collagen I and fibronectin on the adhesion, elasticity and cytoskeletal organization of prostate cancer cells. Biochem. Biophys. Research Comm. 2010; 402:361–366. [PubMed: 20946884]

Feeley BT, Gamradt SC, Hsu WK, Liu N, Krenek L, Robbins P, Huard J, Lieberman JR. Influence of BMPs on the formation of osteoblastic lesions in metastatic prostate cancer. J Bone Miner Res. 2005; 20:2189–2199. [PubMed: 16294272]

Gabbitas B, Canalis E. Insulin-like growth factors sustain insulin-like growth factor-binding protein-5 expression in osteoblasts. Am J Physiol. 1998; 275(2 Pt 1):E222–E228. [PubMed: 9688622]

Gingrich JR, Barrios RJ, Morton RA, Boyce BF, DeMayo FJ, Finegold MJ, Angelopoulou R, Rosen JM, Greenberg NM. Metastatic prostate cancer in a transgenic mouse. Cancer Res. 1996; 56:4096–4102. [PubMed: 8797572]

Hall CL, Dai J, van Golen KL, Keller ET, Long MW. Type I collagen receptor ($\alpha_v\beta_1$) signaling promotes the growth of human prostate cancer cells within the bone. Cancer Res. 2006; 66:8648–8654. [PubMed: 16951179]

Ingram RT, Clarke BL, Fisher LW, Fitzpatrick LA. Distribution of noncollagenous proteins in the matrix of adult human bone: evidence of anatomic and functional heterogeneity. J. Bone Miner. Res. 1993; 8 1019-10122.

Jacob K, Webber M, Benayahu D, Kleinman HK. Osteonectin promotes prostate cancer cell immigration and invasion: a possible mechanism for metastasis to bone. Cancer Res. 1999; 59:4453–4457. [PubMed: 10485497]

Janmey PA, Winer JP, Murray ME, Wen Q. The hard life of soft cells. Cell Motil. Cytoskeleton. 2009; 66:597–605. [PubMed: 19479819]

Jean C, Gravelle P, Fournie J-J, Laurent G. Influence of stress on extracellular matrix and integrin biology. Oncogene. 2011; 30:2697–2606. [PubMed: 21339741]

Kaighn ME, Narayan KS, Ohnuki Y, Lechner JF, Jones LW. Establishment and characterization of a human prostatic carcinoma cell line (PC-3). Invest. Urol. 1979; 17:6–23.

Kalajzic I, Staal A, Yang WP, Wu Y, Johnson SE, Feyen JH, Krueger W, Maye P, Yu F, Zhao Y, Kuo L, Gupta RR, Achenie LE, Wang HW, Shin DG, Rowe DW. Expression profile of osteoblast lineage at defined stages of differentiation. J Biol Chem. 2005; 280:24618–24626. [PubMed: 15834136]

NIH-PA Author Manuscript

NIH-PA Author Manuscript

NIH-PA Author Manuscript

Kapinas K, Kessler CB, Delany AM. miR-29 suppression of osteonectin in osteoblasts: regulation during differentiation and by canonical wnt signaling. J Cell Biochem. 2009; 108:216–224. [PubMed: 19565563]

Kessler CB, Delany AM. Increased notch 1 expression and attenuated stimulatory G protein coupling to adenylyl cyclase in osteonectin-null osteoblasts. Endocrinology. 2008; 148:1666–1674. [PubMed: 17218421]

Kim D-H, Nan K, Gupta K, Kwon KW, Suh K-Y, Levchenko A. Mechanosensitivity of fibroblast cell shape and movement to anisotropic substratum topography gradients. Biomaterials. 2009; 30:5433–5444. [PubMed: 19595452]

Kong Z, Xie D, Boike T, Raghavan P, Burma S, Chen DJ, Habib AA, Chakraborty A, Hsieh J-T, Saha D. Downregulation of human DAB2IP gene expression in prostate cancer cells results in resistance to ionizing radiation. Cancer Res. 2010; 70:2829–2839. [PubMed: 20332235]

Lacomb R, Nadiarnykh O, Campagnola PJ. Quantitative second harmonic generation imaging of diseased state osteogenesis imperfecta: experiment and simulation. Biophys J. 2008; 94:4504–4515. [PubMed: 18281387]

Larsen M, Artym VV, Green JA, Yamada KM. The matrix reorganized: extracellular matrix remodeling and integrin signaling. Current Opinion Cell Biol. 2006; 18:463–471. [PubMed: 16919434]

Lee Y-P, Schwartz EM, Davies M, Jo M, Gates J, Zhang X, Wu J, Lieberman JR. Use of zoledronate to treat osteoblastic versus osteolytic lesions in a severe-combined-immunodeficient mouse model. Cancer Res. 2002; 62:5564–5570. [PubMed: 12359769]

Lin S-H, Cheng C-J, Lee Y-C, Ye X, Tsai W-W, Kim J, Pasqualini R, Arap W, Navone NM, Tu S-M, Hu M, Yu-Lee L-Y, Logothetis CJ. A 45-kDa ErbB3 secreted by prostate cancer cells promotes bone formation. Oncogene. 2008; 27:5195–5203. [PubMed: 18490922]

Machado do Reis L, Kessler CB, Adam sDJ, Lorenzo J, Jorgetti V, Delany AM. Accentuated osteoclastic response to parathyroid hormone undermines bone mass acquisition in osteonectin-null mice. Bone. 2008; 43:264–273. [PubMed: 18499553]

Malaval L, Fournier B, Delmas PD. Radioimmunoassay for osteonectin. Concentrations in bone, nonmineralized tissues, and blood. J. Bone Miner. Res. 1987; 2:457–465. [PubMed: 3455629]

Mannino M, Chalmers AJ. Radioresistance of glioma stem cells: Intrinsic characteristic or property of the “microenvironment-stem cell unit’? Molecular Oncology. 2011; 5:374–386. [PubMed: 21659010]

McCabe NP, Kerr BA, Madajka M, Vasanji A, Byzova TV. Augmented osteolysis in SPARC-deficient mice with bone-residing prostate cancer. Neoplasia. 2011; 13:31–39. [PubMed: 21245938]

Midwood KS, Orend G. The role of tenascin-C in tissue injury and tumorigenesis. J Cell Commun. Signal. 2009; 3:287–310. [PubMed: 19838819]

Moro L, Arbini AA, Marra E, Greco M. Down-regulation of BRCA2 expression by collagen type I promotes prostate cancer cell proliferation. J Biol. Chem. 2005; 280:22482–22491. [PubMed: 15805113]

Nadiarnykh O, Plotnikov S, Mohler WA, Kalajzic I, Redford-Badwal D, Campagnola PJ. Second harmonic generation imaging microscopy studies of osteogenesis imperfecta. J Biomed. Opt. 2007; 12:051805. [PubMed: 17994883]

Pienta KJ, Abate-Shen C, Agus DB, Attar RM, Chung LW, Greenberg NM, Hahn WC, Isaacs JT, Navone NM, Peehl DM, Simons JW, Solit DB, Soule HR, VanDyke TA, Weber MJ, Wu L, Vessella RL. The current state of preclinical prostate cancer animal models. Prostate. 2008; 68:629–639. [PubMed: 18213636]

Podgorski I, Linebaugh BE, Klobinski JE, Rudy DL, Herroon MK, Olive MB, Sloane BF. Bone marrow-derived capthesin K cleaves SPARC in bone metastasis. Am. J. Pathol. 2009; 175:1255–1269. [PubMed: 19700761]

Poincioux R, Lizárraga F, Chavrier P. Matrix invasion by tumour cells: a focus on MT1-MMP trafficking to invadopodia. J. Cell. Sci. 2009; 122:3015–3024. [PubMed: 19692588]

Roudier MP, Morrissey C, True LD, Higano CS, Vessella RL, Ott SM. Histopathological assessment of prostate cancer bone osteoblastic metastases. J Urol. 2008; 180:1154–1160. [PubMed: 18639279]

NIH-PA Author Manuscript

NIH-PA Author Manuscript

NIH-PA Author Manuscript

Robey PG, Boskey AL, Lian JB, Goldring SR. Chapter 3. Extracellular Matrix and Biomineralization of Bone. Primer on the Metabolic Bone Diseases and Disorders of Mineral Metabolism. 2006; 6:12–19.

Sage EH, Reed M, Funk SE, Truong T, Steadele M, Puolakkainen P, Maurice DH, Bassuk JA. Cleavage of the matricellular protein SPARC by matrix metalloproteinase 3 produces polypeptides that influence angiogenesis. J Biol. Chem. 2003; 278:37849–37857. [PubMed: 12867428]

Said N, Frierson HF Jr, Chernauskas D, Motamed K, Theodorescu D. The role of SPARC in the TRAMP model of prostate carcinogenesis and progression. Oncogene. 2009; 28:3487–3498. [PubMed: 19597474]

Sasaki T, Göhring W, Mann K, Maurer P, Hohenester E, Knäuper V, Murphy G, Timpl R. Limited cleavage of extracellular matrix protein BM-40 by matrix metalloproteinases increases its affinity for collagens. J. Biol. Chem. 1997; 272:9237–9243. [PubMed: 9083057]

Shiozawa Y, Pedersen EA, Havens AM, Jung Y, Mishra A, Joseph J, Kim JK, Patel LR, Ying C, Ziegler AM, Pienta MJ, Song J, Wang J, Loberg RD, Krebsbach PH, Pienta KJ, Taichman RS. Human prostate cancer metastases target the hematopoietic stem cell niche to establish footholds in mouse bone marrow. J. Clin. Invest. 2011; 121:1298–1312. [PubMed: 21436587]

Singh, S.; Singh, G. Overview Bone Metastasis: Experimental and Clinical Therapeutics. Singh, G.; Rabbani, SA., editors. Totowa, NJ: Humana Press; 2005. p. 3-12.

Sobel RE, Sadar MD. Cell lines used in prostate cancer research: a compendium of old and new lines-part 1. J Urology. 2005; 173:342–359.

Storch K, Eke I, Borgmann K, Krause M, Richter C, Becker K, Schröck E, Cordes N. Three-dimensional cell growth confers radioresistance by chromatin density modification. Cancer Res. 2010; 70:3925–3934. [PubMed: 20442295]

Sung SY, Hsieh CL, Law A, Zhau HE, Pathak S, Multani AS, Lim S, Coleman IM, Wu LC, Figg WD, Dahut WL, Nelson P, Lee JK, Amin MB, Lyles R, Johnstone PA, Marshall FF, Chung LW. Coevolution of prostate cancer and bone stroma in three-dimensional cocutlure: implications for cancer growth and metastasis. Cancer Res. 2008; 68:9996–10003. [PubMed: 19047182]

Sweeney SM, Orgel JP, Fertala A, McAuliffe JD, Turner KR, Di Lullo GA, Chen S, Antipova O, Perumal S, Ala-Koko L, Forlino A, Cabral WA, Barnes AM, Marini JC, San Antonio JD. Candidate cell and matrix interaction domains on the collagen fibril, the predominant protein of vertebrates. J. Biol. Chem. 2008; 283:21187–21197. [PubMed: 18487200]

Tai IT, Dai M, Owen DA, Chen LB. Genome-wide expression analysis of therapy-resistant tumors reveals SPARC as a novel target for cancer therapy. J. Clin. Invest. 2005; 115:1492–1502. [PubMed: 15902309]

Teixeira AI, Abrams GA, Bertics PJ, Murphy CJ, Nealey PF. Epithelial contact guidance on well-defined micro- and nanostructured substrates. J Cell Sci. 2003; 116:1881–1892. [PubMed: 12692189]

Thomas R, True LK, Bassuk JA, Lang PH, Vessella RL. Differential expression of osteonectin/SPARC during human prostate cancer progression. Clin Cancer Res. 2000; 6:1140–1149. [PubMed: 10741745]

Tilghman RW, Cowan CR, Mih JD, Koryakina Y, Gioeli D, Slack-Davis JK, Blackman BR, Tschumperlin DJ, Parsons JT. PLoS ONE. 2010; 5:e12905. [PubMed: 20886123]

Weidhaas JB, Babar I, Nallur SM, et al. MicroRNAs as potential agents to alter resistance to cytotoxic anticancer therapy. Cancer Res. 2007; 67:11111–11116. [PubMed: 18056433]

Wolf K, Alexander S, Schact V, Coussens LM, von Andrian UH, van Rheenen J, Deryugina E, Friedl P. Collagen-based cell migration models in vitro and in vivo. Seminars in Cell Developmental Biol. 2009; 20:931–941.

Wong SY, Crowley D, Bronson RT, Hynes RO. Analysis of the role of endogenous SPARC in mouse models of prostate and breast cancer. Clin Exp Metastasis. 2008; 25:109–118. [PubMed: 18058030]

Yim EKF, Leong KW. Significance of synthetic nanostructures in dictating cellular response. Nanomedicine. 2005; 1:10–21. [PubMed: 17292053]

Zhang P, Singh A, Yegnasubramanian S, Esopi D, Kombairaju P, Bodas M, Wu H, Bova SG, Biswal S. Loss of kelch-like ECH-associated protein 1 function in prostate cancer cells causes

NIH-PA Author Manuscript

NIH-PA Author Manuscript

NIH-PA Author Manuscript

chemoresistance and radioresistance and promotes tumor growth. Mol. Cancer Ther. 2010; 9:336–346. [PubMed: 20124447]

Zhang W, Pantschenko AG, McCarthy MB, Gronowicz G. Bone-targeted overexpression of Bcl-2 increases osteoblast adhesion and differentiation and inhibits mineralization *in vitro*. Calcif Tissue Int. 2007; 80:111–122. [PubMed: 17308993]

Zhivkova-Galunska M, Adwan H, Eyol E, Kleeff J, Kolb A, Bergmann F, Berger MR. Osteopontin but not osteonectin favors the metastatic growth of pancreatic cancer cell lines. Cancer Biol. Ther. 2010; 10:54–64. [PubMed: 20495387]

NIH-PA Author Manuscript

NIH-PA Author Manuscript

NIH-PA Author Manuscript

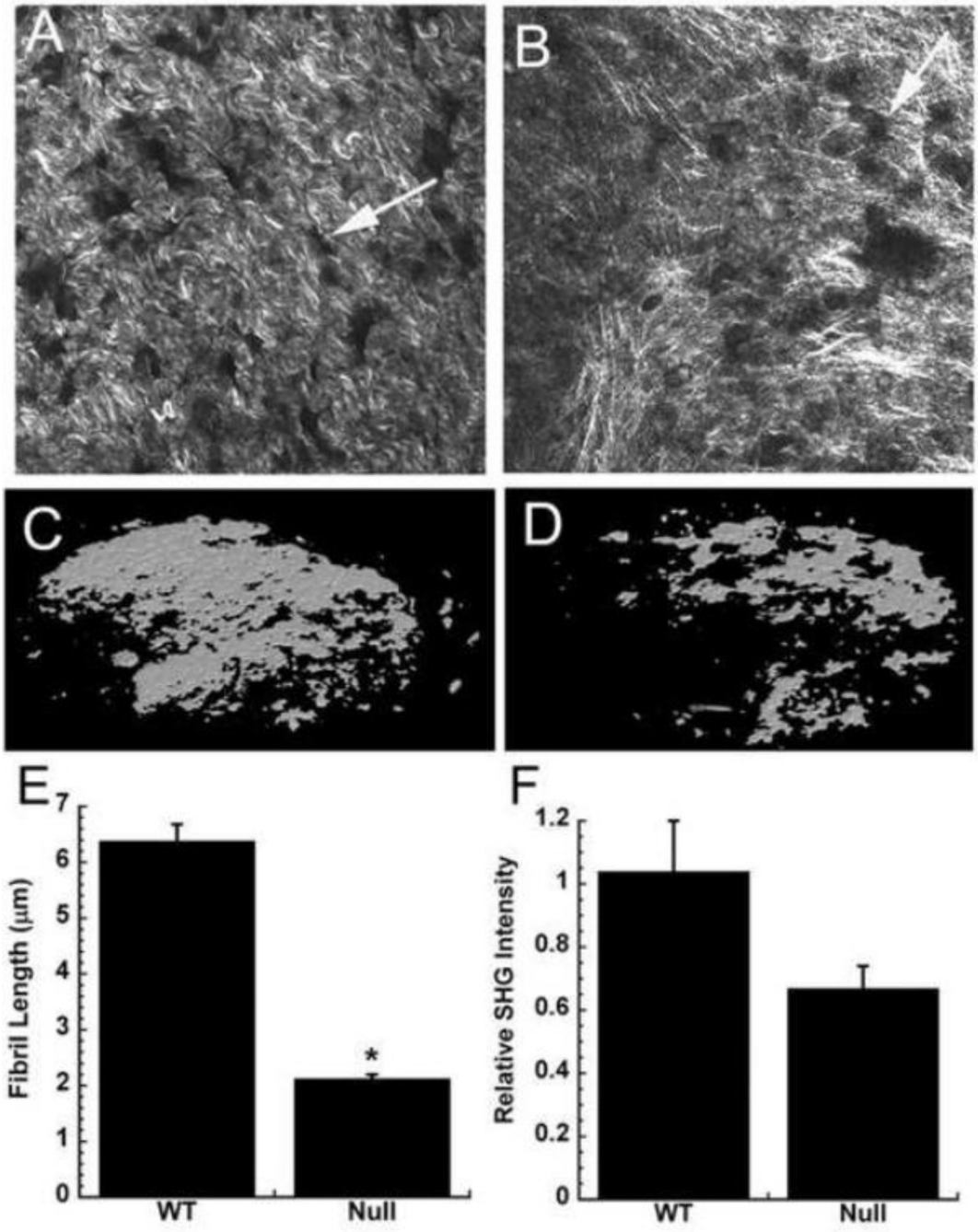

Figure 1. Osteonectin-null bone matrices synthesized in vitro are disorganized and hypomineralized

Collagen fibrer morphology in wild type (A) and osteonectin-null (B) matrices, imaged by SHG (representative fields, individual optical sections). Arrows indicate sites in the matrix formerly occupied by osteoblasts. MicroCT imaging of mineral in wild type (C) and osteonectin-null (D) matrices (representative image of entire well). Collagen fiber length (E) and relative SHG intensity (F) in wild type vs. osteonectin-null matrix. * = significantly different from WT, $p<0.01$.

NIH-PA Author Manuscript

NIH-PA Author Manuscript

NIH-PA Author Manuscript

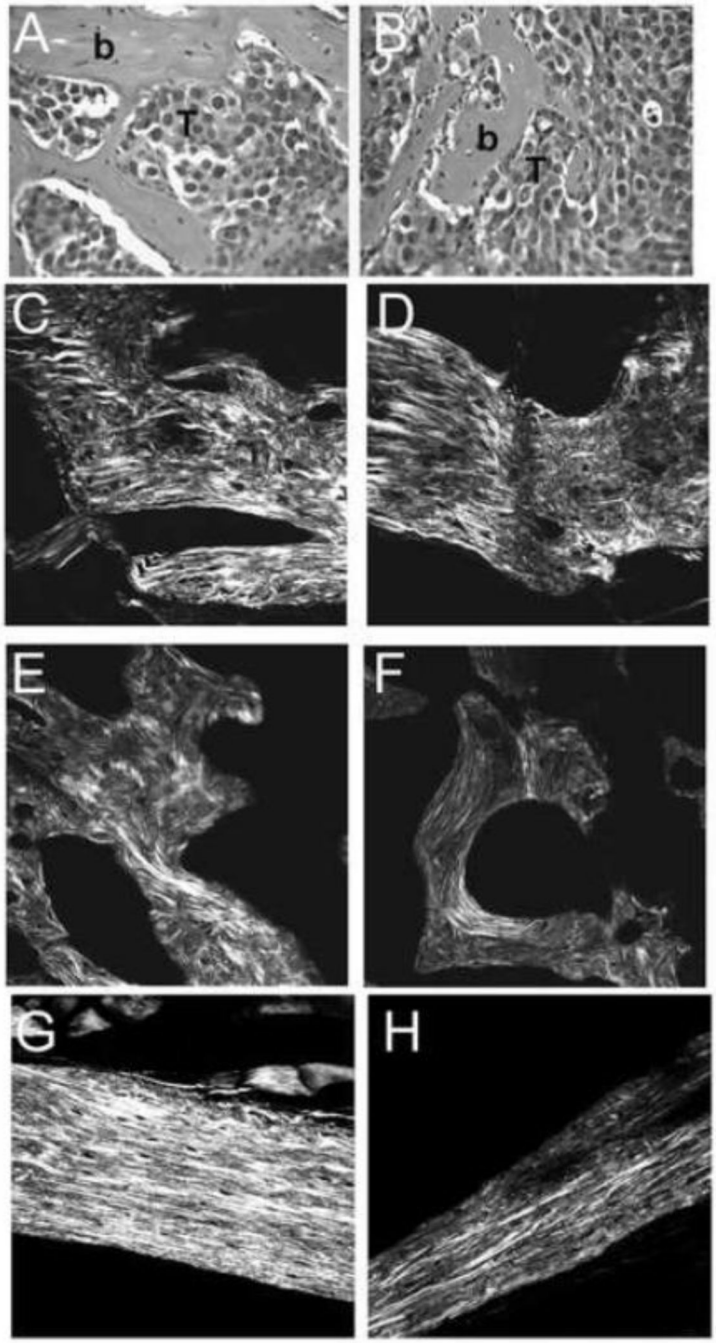

Figure 2. Prostate cancer cell-induced osteoblastic lesions have a woven bone phenotype

Osteoblastic lesion in a mouse tibia injected with LAPC-9 human prostate carcinoma cells: Hematoxylin and eosin staining, where "b" indicates bone and T indicates tumor (A and B). SHG imaging of collagen fibril morphology in osteoblastic lesions (C and D). For comparison, SHG imaging of trabecular bone (E and F) and cortical bone (G and H) in wild type (E and G) and osteonectin-null (F and H) mice. (representative fields, individual optical sections).

NIH-PA Author Manuscript

NIH-PA Author Manuscript

NIH-PA Author Manuscript

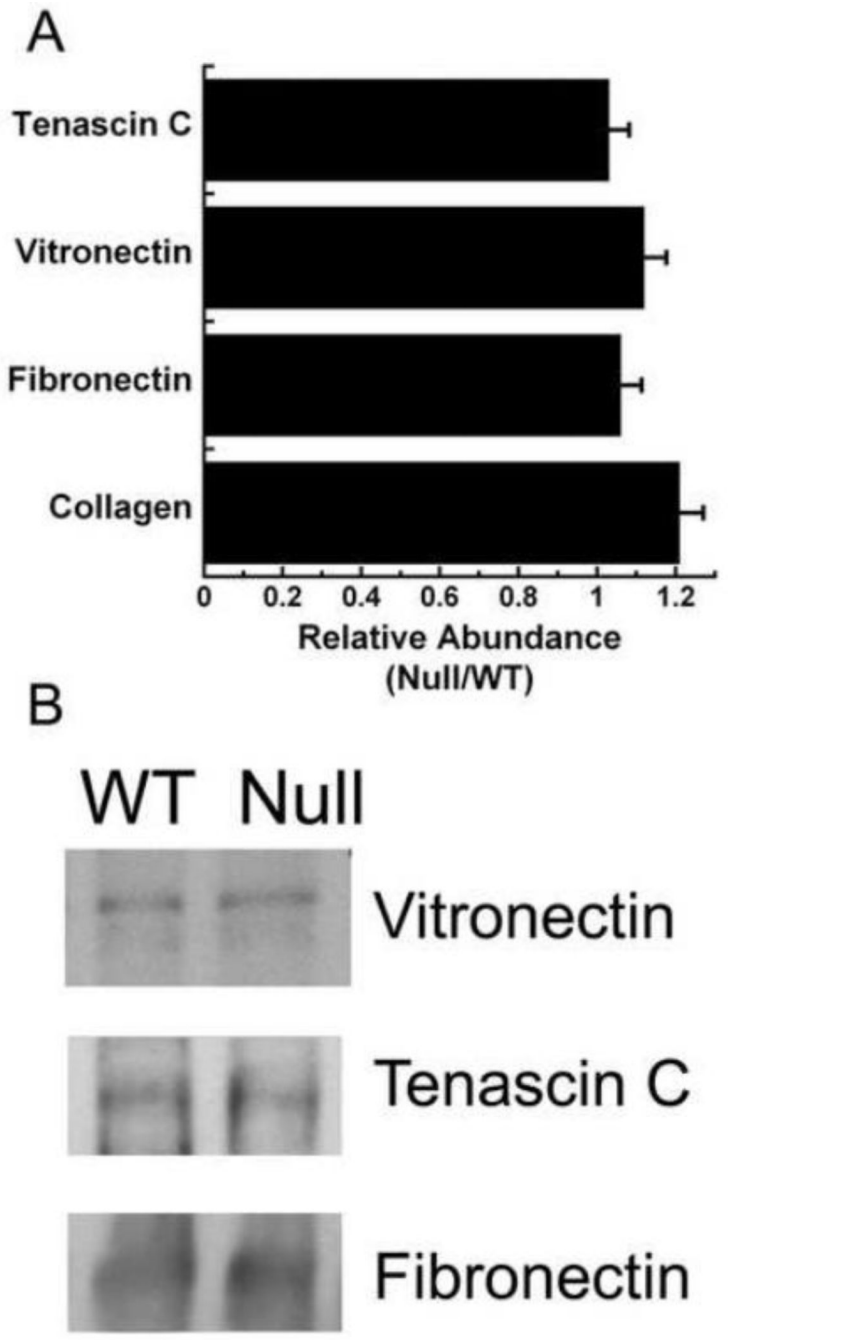

Figure 3. The abundance of selected extracellular matrix proteins is not altered in osteonectin-null matrices

(A) Data for acid soluble collagen was obtained using a Sircol dye binding assay, and data for tenascin C, vitronectin and fibronectin were obtained by Western blot analysis, and representative lanes are shown in (B).

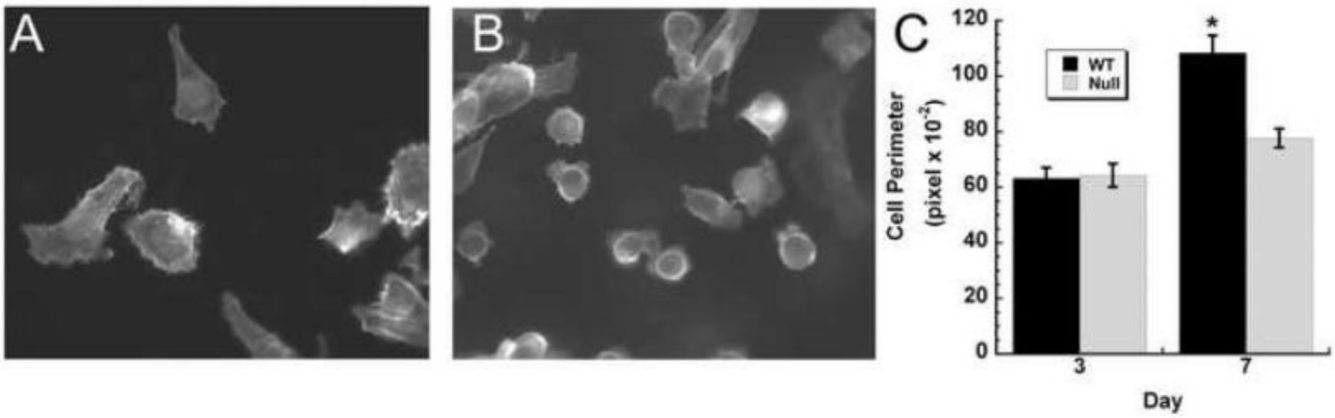

Figure 4. Osteonectin-null matrices impair prostate cancer cell spreading

Representative confocal micrographs of PC-3 cells grown for 7 days on wild type (A) or osteonectin-null matrix (B). Phalloidin and DAPI staining (original magnification 100×). Cell perimeters were quantified, as a measure of cell spreading, after 3 and 7 days of culture (C). * = significantly different from day 3, $p<0.05$.

NIH-PA Author Manuscript
NIH-PA Author Manuscript
NIH-PA Author Manuscript

NIH-PA Author Manuscript
NIH-PA Author Manuscript
NIH-PA Author Manuscript

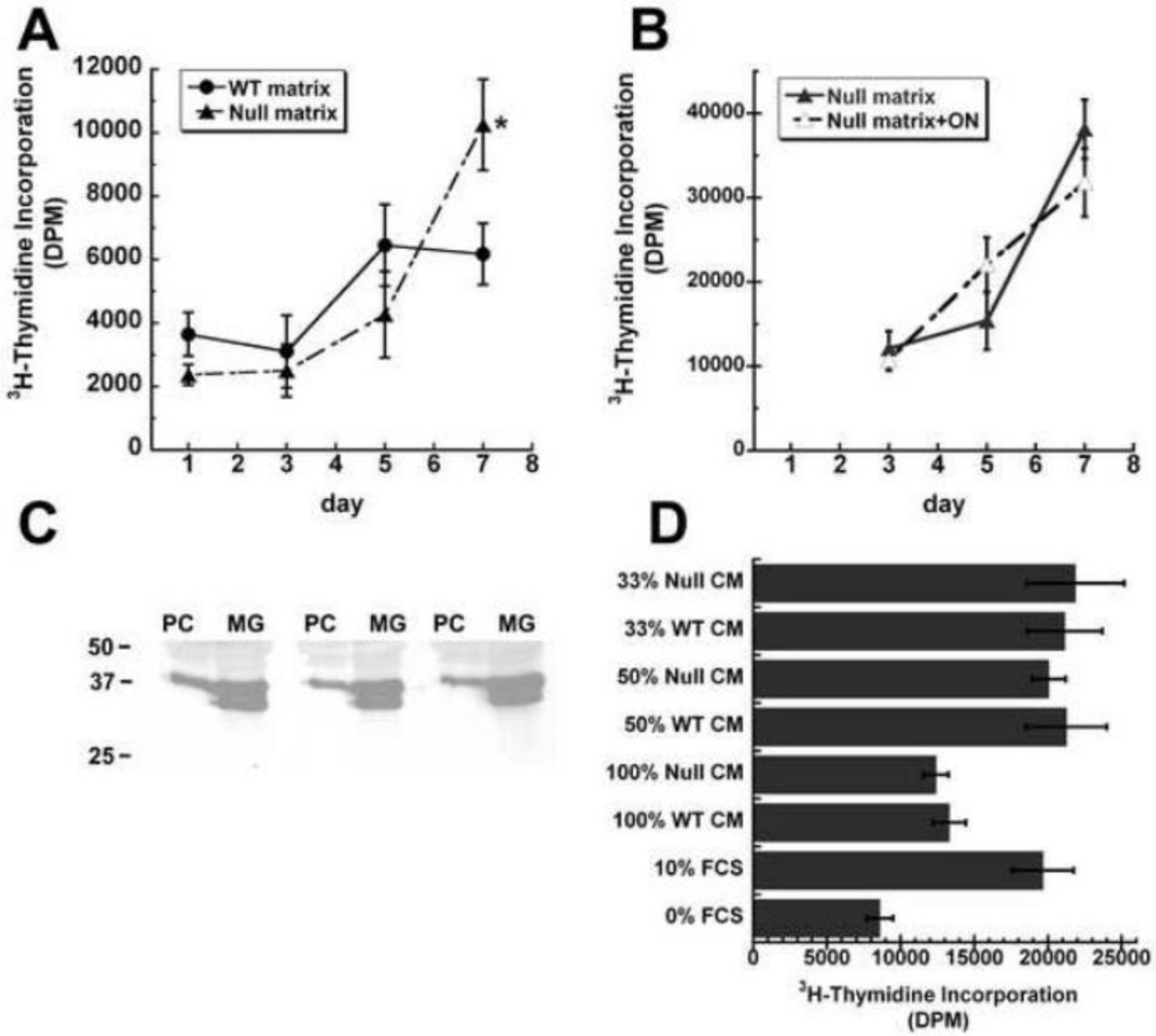

Figure 5. Osteonectin-null bone matrices promote prostate cancer cell proliferation

(A) PC-3 cells were grown on wild type or osteonectin-null matrices, and pulsed with ^{3}H-thymidine on the indicated days. (B) PC-3 cells were grown on osteonectin-null matrices, in the presence or absence of 3 μg/mL recombinant human osteonectin, then pulsed with ^{3}H-thymidine on the indicated days. (C) PC-3 cells (PC) or MG-63 (MG) cells were grown to confluence. Osteonectin in serum-free conditioned medium was analyzed by Western blot analysis. Molecular weight standards (kDa) are indicated on the left of the panel. (D) Serum-deprived cultures of PC-3 cells were treated for 24 hours with conditioned medium from PC-3 cells that had been cultured for 7 days on wild type or osteonectin-null matrices. Cells were then pulsed with ^{3}H-thymidine. Dilutions of medium tested: 100% conditioned medium, 1:2 and 1:3 dilution of conditioned medium in 10% FBS. * = significantly different from WT, $p<0.05$.

NIH-PA Author Manuscript

NIH-PA Author Manuscript

NIH-PA Author Manuscript

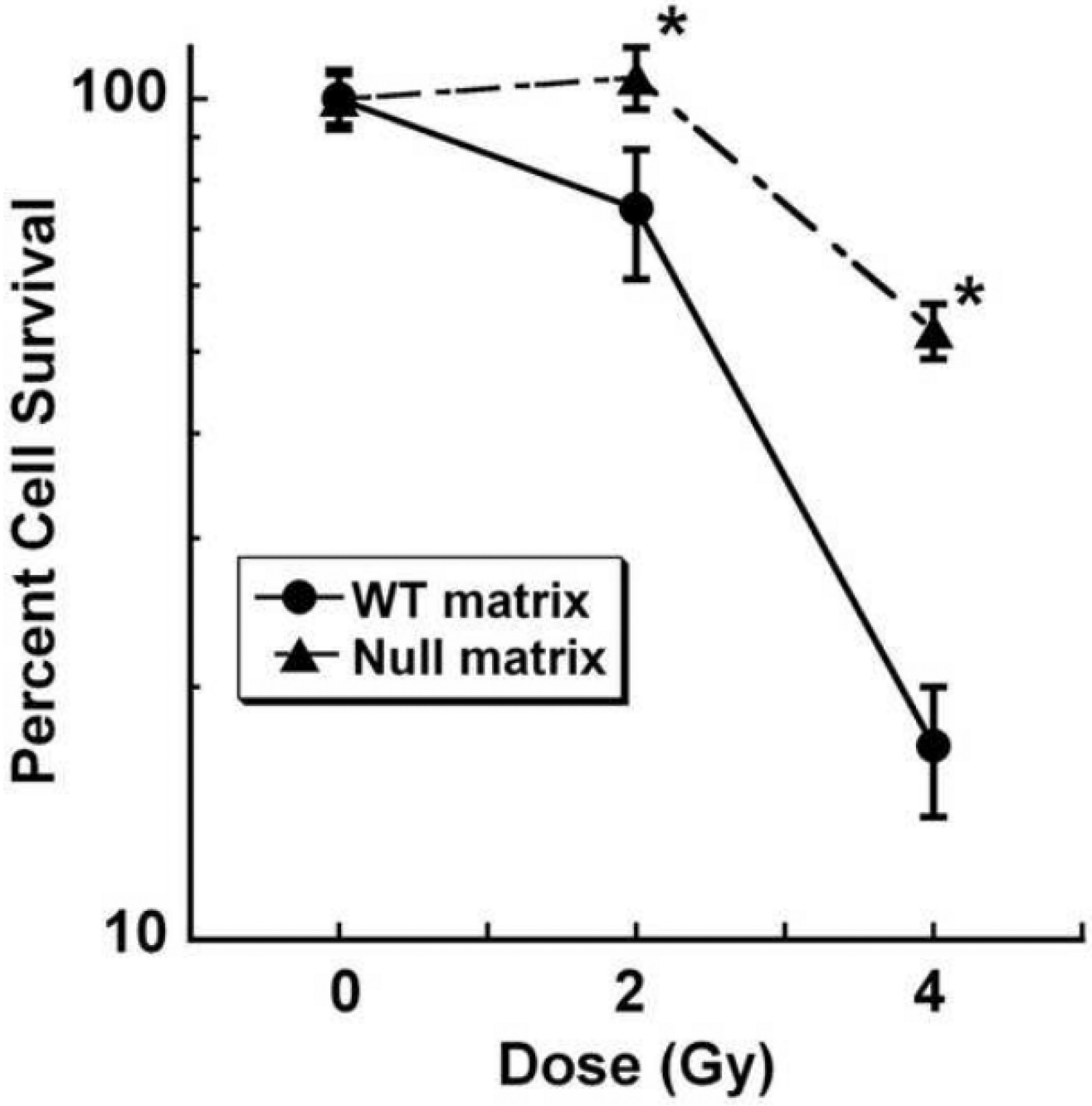

Figure 6. Osteonectin-null bone matrices promote resistance to radiation-induced cell death

PC-3 cells were grown on wild type or osteonectin-null matrices for 6 days, then exposed to 0, 2, or 4 Gy gamma radiation. Cells were re-plated and colony formation was quantified by crystal violet staining. * = significantly different from WT, $p<0.05$.